Environ Monit Assess (2023) 195:1062
https://doi.org/10.1007/s10661-023-11663-2

RESEARCH

Projected climate extremes over agro-climatic zones of Ganga River Basin under 1.5, 2, and 3° global warming levels

Harsh Vardhan Singh · Nitin Joshi · Shakti Suryavanshi

Received: 16 March 2023 / Accepted: 1 August 2023 / Published online: 17 August 2023

Abstract Recurring floods, droughts, heatwaves, and other hydro-meteorological extreme events are likely to be increased under the climate change scenarios. The increased risk of these extreme events might have more exposure to the population; thus, it is important to discuss such extreme events and their projected behavior under a changing climate scenario. In the present study, we have computed the extreme precipitation and temperature indices over the 10 agro-climatic zones falling under the Ganga River Basin (GRB)utilizing a high-resolution daily gridded temperature and precipitation multi-model ensembled CMIP6 dataset (0.25°×0.25°) under global warming levels of 1.5 °C, 2 °C, and 3 °C. We found that the annual daily minimum temperature (TNN) showed a higher rise of about 67% than the maximum temperature (TXX) of 48% in GRB. The basin also experiences a greater increase in the frequency of warm nights (TN90P) of about 67.71% compared to warm days (TX90P) of 29.1% for the 3 °C global warming level. Along with extreme indices, the population exposed due to the impact of the extreme maximum temperature has also been analyzed for progressive warming levels. Population exposure to extreme temperature event (TXX) has been analyzed with 20-year return period using GEV distribution method. The study concludes that the exposed population to extreme temperature event experienced an increase from 46.99 to 52.16% for the whole Ganga Basin. Consecutive dry days (CDD) and consecutive wet days (CWD) both show a significant increasing trend, but CWD has a significant increase in the majority of the zones, while CDD shows a significant decreasing trend for some of the zones for three warming levels periods. Extreme climate indices help to understand the frequency and intensity of extreme weather events such as heavy rainfall, droughts, and heatwaves to develop early warning systems and adaptation strategies to mitigate such events.

Keywords Temperature · Precipitation · Indices · Extreme · CMIP6 · Warming levels

Supplementary Information The online version contains supplementary material available at https://doi.org/10.1007/s10661-023-11663-2.

H. V. Singh · N. Joshi
Department of Civil Engineering, Indian Institute of Technology Jammu, Jammu, India

S. Suryavanshi (✉)
Scientist 'C', National Institute of Hydrology, Roorkee, India
e-mail: suryavanshi.shakti@gmail.com

Introduction

The average temperature of globe has increased since the later half of the last century due to an increase in anthropogenic greenhouse gas emissions (Pachauri et al., 2014a, b). This rising temperature affects the frequency and magnitude of both warm and cold temperature anomalies and furthers various extreme rainfall and temperature events (Diffenbaugh et al., 2005; Seneviratne et al., 2012; Collins et al., 2013). According to the Sixth Assessment Report (AR6) of the IPCC (2022), climate change disproportionately affects local communities that have limited adaptation capabilities (Pörtner et al., 2022). During the last few decades, some unprecedented extreme temperature events like heat waves, wildfires, and winter storms have already intensified throughout much of the world (Handmer et al., 2012). Precipitation extremes can be characterized mainly as floods, caused by exceptionally heavy rainfall, and droughts, caused by abnormally low precipitation and water scarcity; monsoonal downpours, tropical cyclones, heavy deliveries via atmospheric rivers, etc. are influenced by warming trends observed in the global environment (Sen Roy & Balling, 2004; Rao et al., 2014; Zhan et al., 2017; Rai et al., 2020). It has been stated by researchers that there will be an increase in the intensity and variability of the precipitation extreme events with an increase in the warming and GHG concentration in the atmosphere (Akinsanola et al., 2020 and Reddy & Saravanan, 2023).

These temperature extremes have jeopardized not only human health (Haines et al., 2006; Mitchell et al., 2016; Orimoloye et al., 2019; Rahman & Zafarullah, 2020; Tong & Ebi, 2019), agricultural production (Chhogyel & Kumar, 2018; Cogato et al., 2019; Ibn Musah et al., 2018; Sun et al., 2019; Vogel et al., 2019), and economic growth (Burke et al., 2015; Carleton & Hsiang, 2016; Dell et al., 2008, 2012; Moore & Diaz, 2015; Pretis et al., 2018) of various parts of the world but they also disturb various natural ecosystem services (Demertzis & Iliadis, 2018; Mora et al., 2018; Parain et al., 2019; Smale et al., 2019; Stillman, 2019; Vasseur et al., 2014). Extreme temperature and precipitation have the potential to have a negative effect on both the global economy and the standard of living everywhere. The necessary prevention and preparedness to deal with these climate extremes rely on the adaptive capacity of the general population (Mirza, 2003). Many underdeveloped countries located in low-latitude regions, due to their economic, demographic, and geographic reasons, are more vulnerable, incur higher expenses, and have decreased ability to take actions when compared to higher-latitude wealthy countries (Diffenbaugh & Burke, 2019; Mendelsohn et al., 2006).

The development of general circulation models (GCMs) led the researchers to project the future climatic extremes and became helpful in practicing various hydrological models (Mondal et al., 2022). Downscaling of GCMs at the regional level headed to investigate the climatic conditions to finer resolution on the ground. GCMs refer to the time-averaged planetary-scale motion representing the atmosphere's long-term statistical behavior (Mechoso et al., 2015). These are also used to project the anthropogenic GHGs and aerosol impacts on future climate. The sixth phase of Coupled Model Inter-comparison Project (CMIP6) as per including the latest generated Earth System Models compelled by pre-industrial and historical greenhouse gas concentration according to the SSPs. CMIP6 was developed recently as per IPCC Sixth Assessment Report (AR6) and provided a better dataset for various Shared Socioeconomic Pathways (SSPs) under different emission levels (Eyring et al., 2016). Compared to CMIP5 models, CMIP6 models perform better while simulating mean and extreme precipitation (Ayugi et al., 2021), and the performance of climate indices is far better than CMIP5 models in CMIP6. Numerous studies have been carried out to evaluate the extreme climate indices for gridded datasets incorporating the CMIP6 and other GCMs (Akinsanola et al., 2021; Lee et al., 2021; Yue et al., 2021).

From the various modeling approaches and past studies, in many regions, the overnight low temperatures have been raised more than the daytime highs, causing reduction in the diurnal temperature range. It has been discovered that an increase in mean temperature causes less extreme low temperatures and more extreme high temperatures (Meehl et al., 2000). In the global warming scenario, both meridional and vertical temperature gradients are anticipated to change. Climate models show that variations in temperature, particularly temperature gradients, affect atmospheric stability and may have a considerable impact on atmospheric circulation (Cheng-Zhi et al., 2021).

Various studies have been performed in the Indian region regarding the rainfall and temperature changes and their extremes events (Deshpande et al., 2016; Mittal et al., 2014; Nepal & Shreshtha, 2015; Chaubey et al., 2022; Siddha & Sahu, 2022; Koteswara Rao et al., 2022; Rani et al., 2022). The report on the global climate condition in 2015 claims that India and Pakistan jointly reported 4100 deaths due to extremely lethal heatwaves (The Global Climate 2011–2015 (UNFCC), 2016). Over the past four decades, there has been a notable decrease and increase in the average extent and intensity of three-dimensional precipitation occurrences globally over both land and ocean, respectively (Yin et al., 2023). Climate change has been shown to pose significant threats to agriculture, food security, ecosystems, terrestrial water cycle, social economy, and human livelihood standards (Adhikari et al., 2015; Pachauri et al., 2014a, b; Tirado et al., 2010). From various research, it has been concluded that climate extremes are negatively affecting water resources, agriculture, livelihood, biodiversity, vegetation, industries, etc., and these may be responsible for the decline in the economic growth of a region (Planton et al., 2008; Chang-Fung-Martel et al., 2017; Urama et al., 2019; Yehia et al., 2017; Perera et al., 2020; Katopodis et al., 2021; Zhao et al., 2022).

A geographical unit that is uniform in terms of climate and length of the growing season and is climatically suitable for a particular range of crops and cultivars is known as an agro-climatic zone (FAO, 1983). The key components of agro-climatic conditions include classes of soil, temperature, rainfall, and water availability, all of which have an impact on the varieties of flora. The land unit created from an agro-climatic zone superimposed on a landform that modifies the climate and length of the growing season is an agro-ecological zone. India during the seventh planning year (1985–90), under the collaborative project of Planning Commission of India (presently NITI Ayog) and Indian Council of Agricultural Research (ICAR), was classified into fifteen different agro-climatic zones based on the soil, water, rainfall, etc., out of which ten zones fall under the largest river basin of the country. In a country like India, where there are many people living in close quarters, agriculture provides an essential source of income for more than 57% of all households (Dagar et al., 2021). The previous studies which have been carried out on the extreme climatic events in India and particularly the Ganga River Basin are done normally by classifying the regions or unitedly over the regions (Deshpande et al., 2016; Sheikh et al., 2015; Maurya et al., 2023; Yadav et al., 2020; Mishra et al., 2022), but none of the studies have reported the extreme events by classifying the region concerning the agro-climatic zones for projected extreme events. River Ganga and its tributaries have formed the largest range of plain fertile in the country which also provided abundant water resources, fertile soil, and appropriate climatic conditions for highly advanced agriculture-based civilization. The study along with the agro-climatic zones will aid in understanding the predicted patterns of extreme occurrences for stakeholders and policymakers, which will be beneficial for agricultural crops, livelihood, and livestock.

Several studies reported a significant increase in the exposure to the population due to extreme climatic events regionally and across the globe (Chen & Sun, 2019, 2020, 2021; Jones et al., 2015; Rohat et al., 2019; Smirnov et al., 2016; Weber et al., 2020). Chen & Sun, 2020 reported a thrice increase in the exposure to projected extreme precipitation events in urban areas due to rapid urbanization in the future. Droughts with extreme temperature events (i.e., heatwaves) are the most substantial events that affect population exposure (Das et al., 2022). Global population data contains different pathways having their own significance such as SSP1 (sustainability) along with SSP5 (fossil fuel development) accepted as low population growth. SSP1 and SSP5 are considered for medium economic growth and high economic growth, respectively. SSP2 (middle of the road) is accepted as having medium growth in population, urbanization, and economic growth while SSP3 has a high population and economic development with optimum urbanization (Jones & O'Neill, 2016). Under different climate change scenarios, the Ganga River Basin (GRB) is one of the river basins which is most vulnerable to extreme events. Being the most populated and largest river basin in India, it is evident that a large portion of the population of India is affected by climate extremes in the basin. Ganga River Basin due to its varying physiological conditions experiences several extreme climatic events, for example, cloudbursts (Mishra et al., 2022), rainfall extremes (Swarnkar et al., 2021), droughts (Bhatt et al., 2022), and avalanches (Thayyen et al., 2021). Therefore, it is essential to study the impact of temperature extremes on the population of the region as humans are negatively affected in every aspect socially and economically. Agriculture is the most affected regime as it is highly vulnerable to climate extremes. The objective of the present study is to analyze the spatial variability of temperature and precipitation extremes for the projected duration under 1.5, 2, and 3 °C global warming levels over GRB. It also seeks to examine how the population is exposed to the maximum temperature throughout the region and area for a projected period under 1.5, 2, and 3 °C global warming level (GWL).

Study area

The present study is carried out over the Ganga River Basin which includes 11 Indian states. The Ganga River Basin lies between 21° 53′ N to 31° 46′ N latitude and 73° 38′ E and 89° 09′ E longitude. The region has a wide variability in climate and elevation that covers the mountainous, flat, and fertile land of North India. The elevation profile ranges from 100 to 7800 m above average sea level. It covers approximately 8,49,000 km^2 geographical area and a length of 2525 km. In our study, the entire basin is classified into ten agro-climatic zones (Table 1) based on weather patterns and agricultural output, where agricultural land accounting almost 65% land of the total area. Based on homogeneity in rainfall, temperature, topography, crops and agricultural systems, and water resources, the nation was divided into various agro-climatic zones out of which Ganga River Basin is shown in Fig. 1. The GRB comprises a large variety of land use classes from which agricultural land dominates with 65.57% of the geographical area. The basin is rich in soil nutrients and minerals with alluvial soil extending to 52% of the total area, which makes it most fertile basin in India.

GRB is also known for its snow and glacier repository which is important for water resources and hydropower generation. The monsoon season in the basin runs from June to September, rainfall predominates during this time, and the basin ranges from sub-humid to hot and humid climatic conditions. The mean annual rainfall over the basin is about 1059.74 mm with average annual maximum and minimum temperatures of about 32.05 °C and 18.44 °C, respectively. The river Ganga comprises tributaries, i.e., Alaknanda, Bhagirathi, Yamuna, Gomti, and Betwa rivers, and flows approximately 2525 km up to outfall at the Bay of Bengal.

Datasets used

In the present study, daily gridded precipitation data were obtained from India Meteorological Department (IMD), at a grid size of 0.25°. Since temperature data from IMD is not available at the same resolution of rainfall, therefore, minimum and maximum daily temperature dataset at 0.25° spatial resolution provided by the Terrestrial Hydrology Group at Princeton University (Sheffield et al., 2006) has been used in this study. These were observed datasets for the base period of 1971 to 2000. High-resolution bias-corrected daily precipitation, minimum and maximum temperature CMIP6 datasets, provided by Mishra et al. (2020a, b) for 13 models, and four shared socio-economic pathways (SSPs), i.e., ssp126, ssp245, ssp370, and ssp585 for the period of 2001 to 2100, have been used. They used the statistical bias-correction method to remove the exhibit systematic biases present in the datasets with the help of Empirical Quantile Mapping (EQM) to downscale the temperature and precipitation. They found that EQM successfully removed the biases in both mean and extreme precipitation and minimum and maximum temperature. The details of the GCM

Table 1 List of agro-climatic zones in Ganga River Basin

Zone no	Description about the zone	Area (in sq. kms)	Area (%)
1	Western Himalayan Region	59,392.79	7
2	Eastern Himalayan Region	1470	0.17
3	Lower Gangetic Plain Region	62,672	7.4
4	Middle Gangetic Plain Region	173,535.1	20.3
5	Upper Gangetic Plain Region	145,820.7	17.2
6	Trans Gangetic Plain Region	14,807.33	1.76
7	Eastern Plateau and Hills Region	95,702.76	11.28
8	Central Plateau and Hills Region	253,533	30
9	Western Plateau and Hills Region	38,642	4.5
10	Western dry region	3316.912	0.39

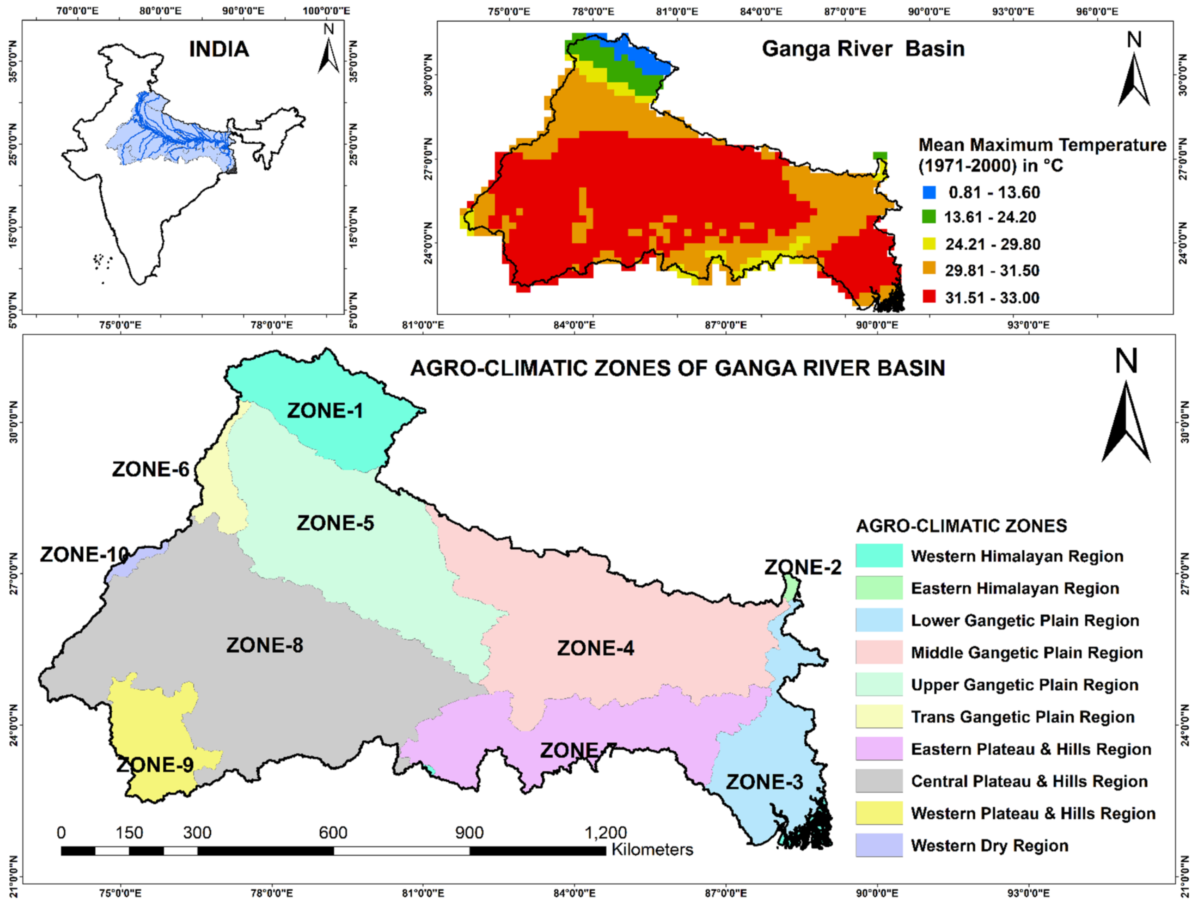

Fig. 1 Map of the study area showing the Ganga River Basin and different agro-climatic zones in it (source: India-Water Resources Information System)

datasets along with their warming levels are presented in Fig. S1. To check the accuracy of the GCM models, percent bias has been computed for the period of 1971 to 2000 for both GCM models and observed datasets. Here, we have calculated the percent bias for individual GCM models (Fig. S2) and for the ensemble mean of GCM models with respect to observed precipitation (Fig. S3). Figure S4 represents the Taylordiagram of the bias-corrected temperature dataset of all 13 GCMs with reference to the observed dataset in which minimum temperature (Fig. S3a) shows correlation ranges between 0.72 and 0.76 and maximum temperature (Fig. S3b) shows the correlation of about 0.74 to 0.78, and Fig. S5 shows Taylor-diagram for the precipitation dataset of all GCMs used in the study with respect to the observed precipitation having a good correlation between 0.70 and 0.72. The results show a very good correlation between the observed and GCM datasets with very less percent-bias values. However, to see the inter-climate model differences and uncertainty, we have also plotted the yearly mean of the minimum and maximum temperatures (Fig. S6) and precipitation (Fig. S7) for the base period (1971–2000) of all 13 models with respect to the observed dataset, which shows small deviations from the observed dataset.

We have used the gridded population datasets for the four SSPs to examine how excessive temperature affects the population. NASA's Socioeconomic Data & Applications Centre is the source from where population datasets for the years 2000 to 2100 (Jones & O'Neill, 2016; Russo et al., 2019; Gao, 2020) were acquainted. To align with the IMD grids, the population dataset was regridded at a spatial resolution of 0.25°. The data is linearly interpolated to the annual time step because it is available at 10-year intervals. The population base period was considered as of the year 2000 for the study.

Methodology

Environmental consequences are frequently caused by short-term occurrences that occur well into the distribution tails of daily data, even though monthly means offer useful climatological information to detect sluggish changes in climate trends (Zhang et al., 2018). Thus, the Expert Team on Climate Change Detection and Indices (ETCCDI) developed a core set of 27 indices to provide a unified perspective on observed shifts in weather and climatic extremes. These indices are intended to track variations in the frequency and severity of "moderately" extreme occurrences by concentrating on those that generally happen several times a year as opposed to highly significant weather events that only occur for a long duration of time (Yosef et al., 2019). From the set of 27 defined extreme weather and climate indices, we have used four for each (i.e., temperature and precipitation), totaling eight indices in our study (Table 2).

In the present study, we computed the extreme temperature and precipitation indices for each SSP, and then, the warming-wise multi-model ensembled arithmetic mean of the indices was taken to reduce the wide uncertainty associated with the CMIP6 GCMs (Ma & Yuan, 2021) used in the study. Further, extreme indices of the base period were subtracted from the ensemble mean of different warming levels. The grids with significant increasing and decreasing trends were estimated using the *t*-test (Haan, 1977) as it gives a better trend for slope (magnitude)-based analysis and is more suitable for hydro-meteorological studies (Yue & Pilon, 2004).

Extreme temperature and precipitation indices

Extreme temperature indices defined by ETCCDI (Zhang et al., 2011a, b) were used in the study, which is calculated using daily minimum and maximum temperature data for both observed (1971–2014) and projected (2015–2100) length of duration.

Extreme precipitation indices were also calculated in the present study using daily precipitation data for observed and projected periods. Four precipitation indices were used in the study, i.e., PCPTOT (annual total precipitation in wet days), R95P (annual total precipitation when daily precipitation amount on a wet day > 95th percentile), CWD (maximum number of consecutive wet days), and CDD (maximum number of consecutive dry days).

Estimation of 1.5°, 2°, and 3° global warming level period

For the calculation of 1.5°, 2°, and 3° global warming level periods for different GCMs, we analyzed a time frame of 30 years and calculated the temperature anomalies globally relative to the reference period of 1971–2000 found to be 0.46 °C warmer than pre-industrial global mean temperature based on observational datasets. This warming value for the base period has been taken as a reference and analyzed that global mean temperature in which of the 30-year period GCMs reaches 1.04 °C, 1.54 °C, and 2.54 °C for getting 1.5 °C, 2 °C, and 3 °C warming scenarios, respectively (Marx et al., 2018; Schleussner et al., 2016; Singh & Kumar, 2019; Vautard et al., 2014).

Table 2 List of extreme indices used in the study

Category	Indices	Description	Units
Temperature Indices	TXX	Maximum value of daily maximum temperature	°C
	TX90P	Percentage of days when TX > 90th percentile	%
	TNN	Minimum value of daily minimum temperature	°C
	TN90P	Percentage of days when TN > 90th percentile	%
Precipitation Indices	PCPTOT	Annual total precipitation in wet days	mm
	R95P	Annual total precipitation when RR > 95th percentile	mm
	CWD	Maximum number of consecutive wet days	Days
	CDD	Maximum number of consecutive dry days	Days

Avoided impact of global warmings

Avoided impacts for two scenarios have been considered in the present study for each of the indices to avoid the extreme events at 1.5 °C and 2 °C warmer climates compared with impacts of 2 °C and 3 °C warmer climates (Frame et al., 2017; Li et al., 2018; Nangombe et al., 2019; Zhang et al., 2018). Avoided impact is the exposure that could be avoided by mitigating the future levels of climate change and quantifying the dependence of the exposure on population outcomes. It may be used to quantify the difference between two warming levels in terms of percentage with respect to the base period. The avoided impact for both cases was calculated using the equations given below:

$$\text{Avoided Impact} - 2(\text{AI} - 2) = \frac{\Delta 2°\text{C} - \Delta 1.5°\text{C}}{\Delta 2°\text{C}} \times 100\%, \quad (1)$$

$$\text{Avoided Impact} - 3(\text{AI} - 3) = \frac{\Delta 3°\text{C} - \Delta 2°\text{C}}{\Delta 3°\text{C}} \times 100\% \quad (2)$$

where Δ in the equations above represents the change in the extreme events concerning the base period, i.e., Δ1.5 °C means the difference between extreme events in a 1.5 °C warming level and the base period (1971–2000). If we are talking about the AI-2, then it means the extreme high-temperature events are avoided at 1.5 °C compared to the 2 °C warmer climate. By using this, we can assess the percentage reduction in the impact of climate change by aiming for a target of limiting global temperature increase to 1.5 °C instead of 2 °C. The higher the percentage, the greater the avoided impact, indicating a more ambitious and effective climate mitigation effort.

Population exposure

Population exposure refers to the extent to which a population is subjected to a specific factor or condition, typically referring to potential risks or influences that may affect the health, well-being, or experiences of individuals within that population. It represents the level of contact or interaction between a population and a particular phenomenon, such as environmental hazards, disease outbreaks, pollutants, or social determinants of health. Population exposure can be measured and assessed in various ways, depending on the specific context. It involves considering factors such as the duration, intensity, and frequency of exposure, as well as the size and characteristics of the population at risk.

Among the eight indices used in the study, we have selected TXX, extreme indices as TXX specifically focuses on maximum temperature extremes, which can significantly impact human health and well-being. Heatwaves and extremely high temperatures pose substantial risks to vulnerable populations, such as the elderly, children, and those with pre-existing health conditions. TXX has been used in numerous studies globally, i.e., Jones et al., 2015; Dosio et al., 2018; Li et al., 2019; Iyakaremye et al., 2021; Tuholske et al., 2021, allowing for the comparisons across different regions and time-periods.

Here, we have calculated the return period value of TXX using the generalized extreme value (GEV) distribution method for 20 years. Population data were gridded at a grid size of 0.25° resolution using Climate Data Operator (CDO) and then interpolated to yearly data from the year 2001 to 2100. Population exposure was calculated using return value, population data, and indices (TXX) warming-wise for each model. To calculate the population exposure for an extreme temperature event (TXX) using the provided data, we have used the following relationship:

$$\text{Population Exposure} = (\text{TXX}) \times 20 \text{ year return value} \times \text{Population} \quad (3)$$

We have estimated the avoided impacts 2 and 3 for the population exposure similarly as mentioned in Eqs. (1) and (2). The avoided impact on the areal exposure for the GRB has also been calculated as the product of the number of exposed grids and the area of a single grid.

Results

Indices performance over 1.5, 2, and 3 °C GWL

Temperature indices

Figure 2 shows the spatial plot of extreme temperature indices used in the study, and the indices were presented for additional warming of 1.04 °C

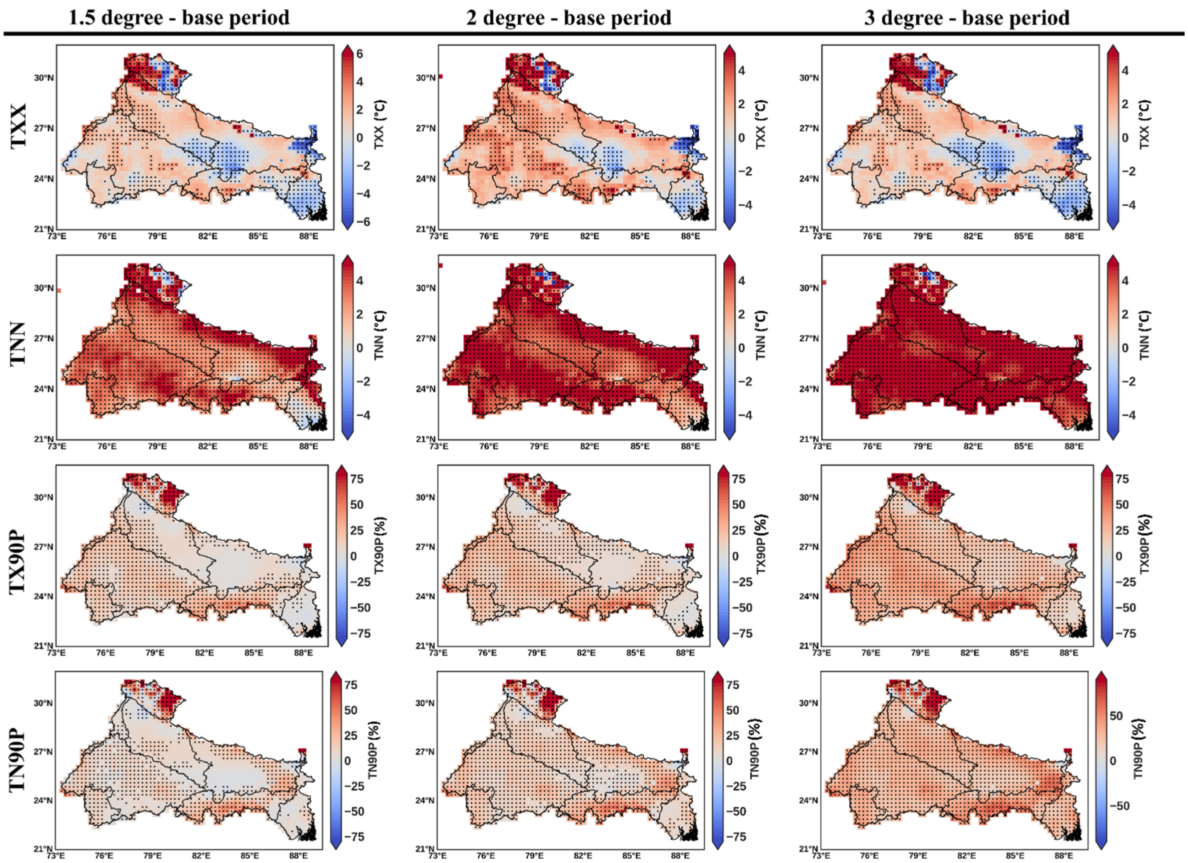

Fig. 2 Spatial distribution of change in temperature climate extremes under 1.5 °C (column-I), 2 °C (column-II), and 3 °C (column-III) GWL with respect to base period (1971–2000). The dotted points are showing 75% of model's grids significantly change with 95% confidence level based on the *t*-test

(1.5 °C-base period), 1.54 °C (2 °C-base period), and 2.54 °C (3 °C-base period) for the 30-year duration. For 1.5 °C GWL, TXX has an average value of 0.9516 for GRB, which has increased about 44% in 2 °C-base period GWL and to 48% in 3 °C-base period GWL in respect of the 1.5 °C GWL, with an increase in the number of significant grids showing changes over a major area of the basin. Figure 2 shows that Zone-1 experiences a significant rise in the index compared to the other zones. TX90P has increased by 13.406% at 1.5 °C, 25.60% at 2 °C, and 53.93% at 3 °C. TN90P value is 10.44% at 1.5 °C, which has ascended to 37.48% at 2 °C and around 67.71% at 3 °C.

TNN mean value for GRB at 1.5 °C GWL is 3.6 °C, which increases with an increase in warming levels and reached 5.1 °C at 3 °C GWL. TNN has increased 28.02% and 40.39% at 2 °C and 3 °C, respectively with respect to 1.5 °C GWL. TNN has the highest increase in Zone-1 and the lowest in Zone-3, yet TNN was found to have a significant increase in more than 95% of grids of the GRB for all the warming levels. TX90P has the averaged basin value of 13.46%, 18%, and 29.1% at 1.5 °C, 2 °C, and 3 °C GWLs, respectively. A significant rise in TX90P was observed in Zone-1 in all three warming levels and it is evident that the number of significant grids are increasing with the increase in warming levels in the GRB.

Precipitation indices In Fig. 3, warming-wise extreme precipitation indices were calculated, and their ensemble spatial plots by detracting with baseline (1971–2000) are presented for three global warming scenarios, i.e., 1.5, 2, and 3 °C GWLs of 30-year duration each.

The magnitudes of the mean PCPTOT of GRB were found to be 473.61 mm, 755.69 mm, and

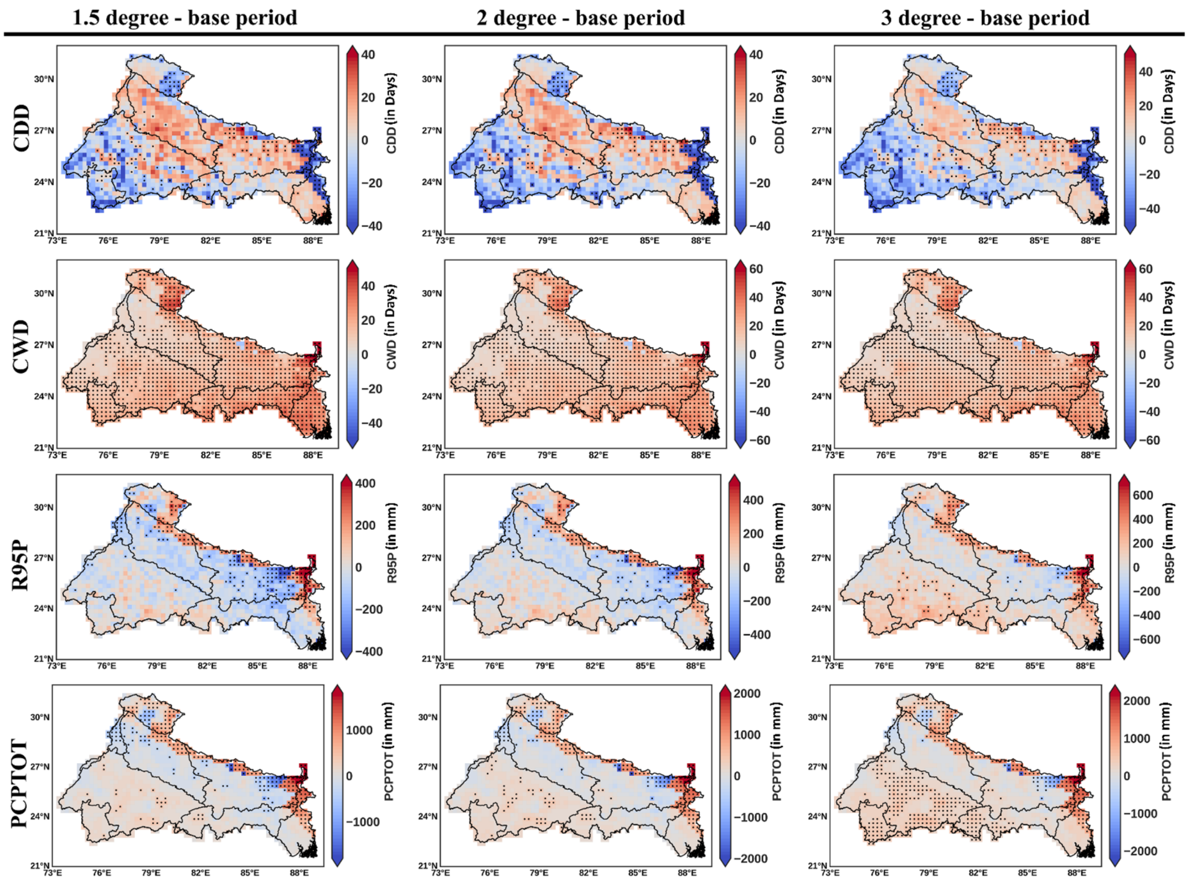

Fig. 3 Spatial distribution of change in precipitation climate extremes under 1.5 °C (column-I), 2 °C (column-II), and 3 °C (column-III) GWL with respect to the base period (1971–2000). The dotted points are showing 75% of the model's grids significantly change with a 95% confidence level based on the *t*-test

861.93 mm for 1.5, 2, and 3 °C GWLs, respectively. Zones 1, 2, 3, 4, and 5 are showing a significant increase in the total precipitation value while the rest of the zones are showing a declining trend of PCPTOT. R95P was found to have a significant increase in the GRB with a mean of 8.51 mm, 15.74 mm, and 27.84 mm at 1.5, 2, and 3 °C GWLs, respectively. R95P found a significant increase in zones 1, 2, 3, 4, and 5 while decreasing in other zones. CWD for 1.5, 2, and 3 °C GWLs was about 10.41, 13.79, and 15.75 days, respectively, which was found significantly rise in zones 1, 7, 3, and 2 while decreasing in the remaining zones. Consecutive dry days (CDD) were found to increase with the increase in warming level, CDD was found at about 13.64, 18.45, and 25.32 days for 1.5, 2, and 3 °C GWLs, respectively. CDD shows a significant rise in zones 4, 5, 8, and 10.

Avoided impact of indices over GRB

Avoided impact (AI) for 2 and 3 °C GWLs has been calculated, and then, the bootstrapping has been implemented over these avoided impacts with 10% and 90% values, which are shown in Figs. 4 and 5 for different indices. Bootstrapping is a resampling technique used to estimate the sampling distribution of a statistic or to make inferences about a population from a sample. It is a powerful technique that allows researchers to assess the variability and uncertainty associated with the estimates (Panagoulia et al., 2014; Parey et al., 2010; Strauss et al., 2013). It works on creating a large number of resamples, from the original dataset. Avoided impact of the extreme temperature indices over the GRB is shown in Fig. 4. Here, avoided impact reduced to 0.5 °C (AI-2) and 1 °C (AI-3) has been

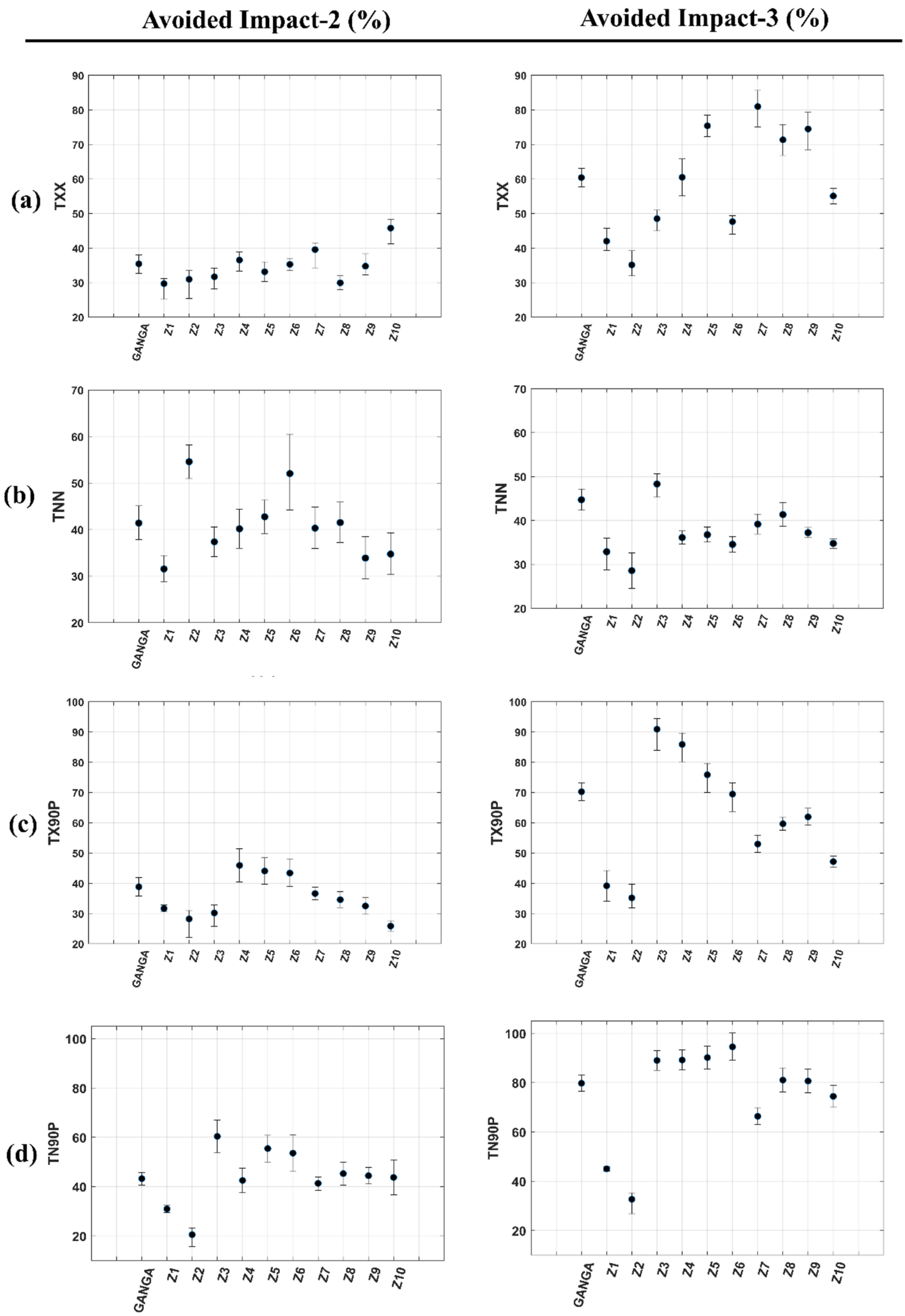

Fig. 4 Projected avoided impact of climate extremes across Ganga River Basin and agro-climatic zones TXX, TNN, TX90P, and TN90P. Solid circles represent the mean value of the indices, and the bars show 10- and 90-percentile values derived from bootstrapping

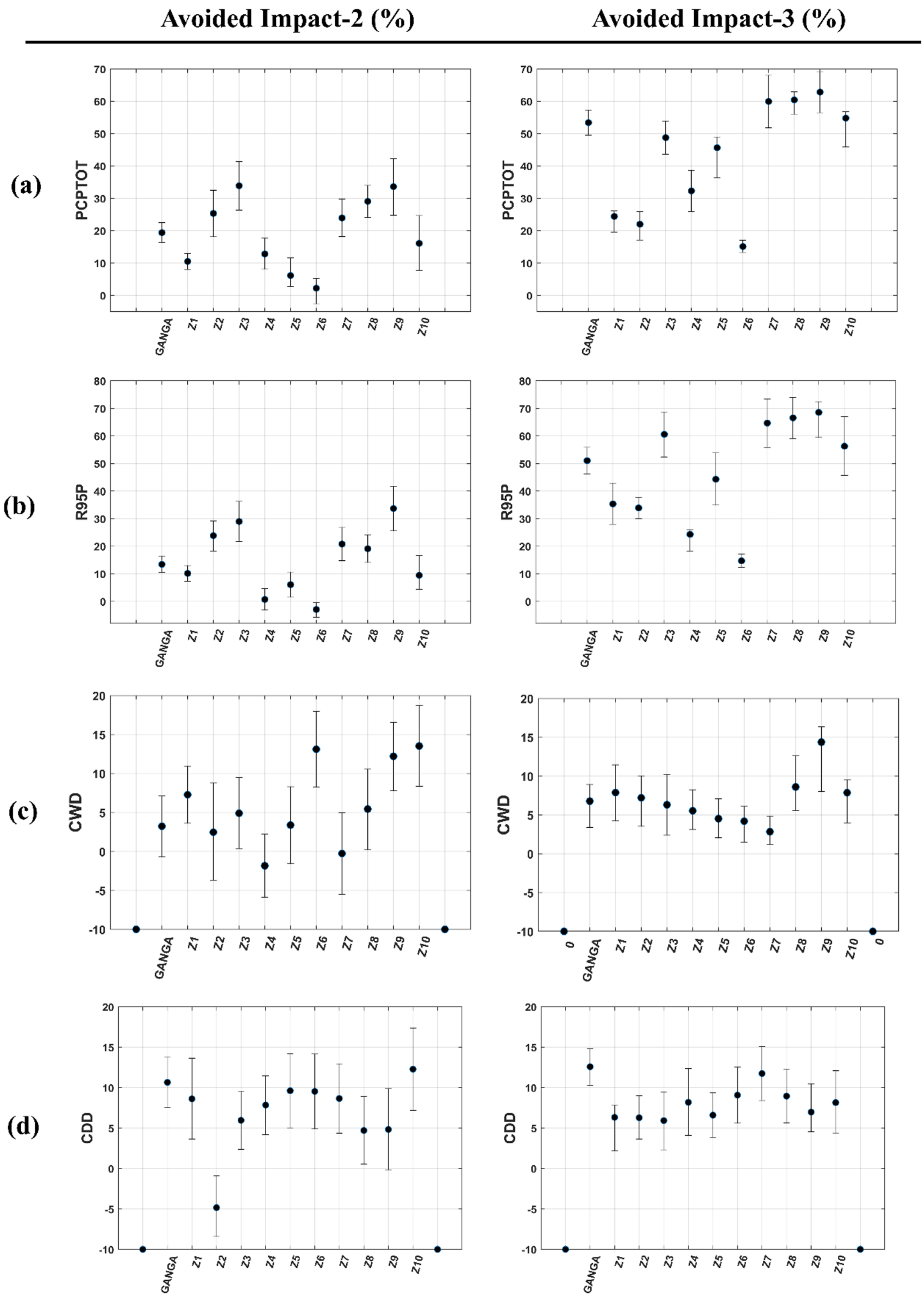

Fig. 5 Projected avoided impact of climate extremes across Ganga River Basin and agro-climatic zones PCPTOT, R95P, CWD, and CDD. Solid circles represent the mean value of the indices, and the bars show 10- and 90-percentile values derived from bootstrapping

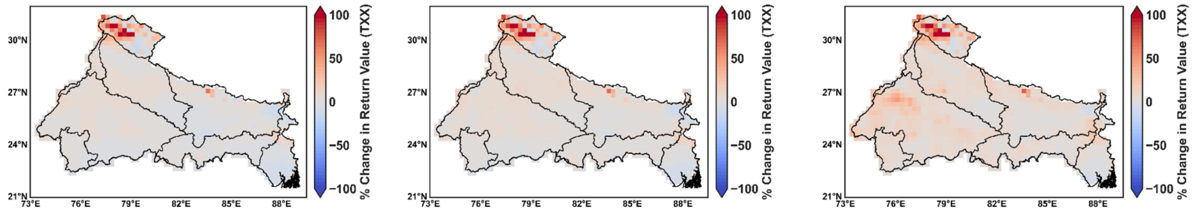

Fig. 6 Spatial distribution of percentage change in return value for the 20-year period of TXX under 1.5 °C (column-I), 2 °C (column-II), and 3 °C (column-III) GWL with respect to the base period (1971–2000)

presented for each index. From the figure, it is visible that TXX has significantly increased in AI-3 concerning AI-2 from 35 to 60% in GRB.

TX90P has increased from 38.82 to 70.27% in AI-3, and a major increase has been observed in Zone-3. TNN has been presented which shows a slight change from 41.39 to 44.71% overall of the basin, and Zone-2 has a prominent decrease from 54.58 to 28.57%. TN90P is projecting an increase from 43.20 to 79.72% from AI-2 to AI-3 in which Zone-2 shows an astonishing rise of about 59.34%.

Figure 5 shows the avoided impact of precipitation extremes for additional 0.5 and 1 °C warming levels. From the figure, it can be seen that PCPTOT average value over the GRB increased to 13.43% in AI-2 and reached 53.41% in AI-3. R95P presented in the figure shows that aggregated mean value of the index reached 13.43% to 51.04% in GRB from AI-2 to AI-3, respectively. Zones 7, 8, 9, and 10 showed a higher upswing in the R95P index value in comparison to other zones. From the figure, the mean extreme CWD values rise from 7.39 (AI-2) to 8.83% in AI-3 for the GRB. CWD has the highest value for Zone-2 and the lowest value for Zone-10 in both circumstances. The average CDD value for the GRB is 8.13% for AI-2 and 8.89% for AI-3 with Zone-2 devising the lowest value and Zone-10 having the highest value of this extreme precipitation index.

Population exposure

Before moving towards the population exposure, the spatial distribution of percentage changes in the return value for the 20-year period of TXX under 1.5 °C, 2 °C, and 3 °C GWL with respect to the base period (1971–2000) is estimated and presented in Fig. 6. It is evident from the figure that the return value of the TXX is reportedly increasing with an increase in warming levels. It also reveals that a higher percentage of the return value is observed for Zone-1 in all three GWLs, while a slight increase in the return value percent change is seen in Central Plateau and Gangetic Plain regions mainly, i.e., zones 4, 5, 8, and 10.

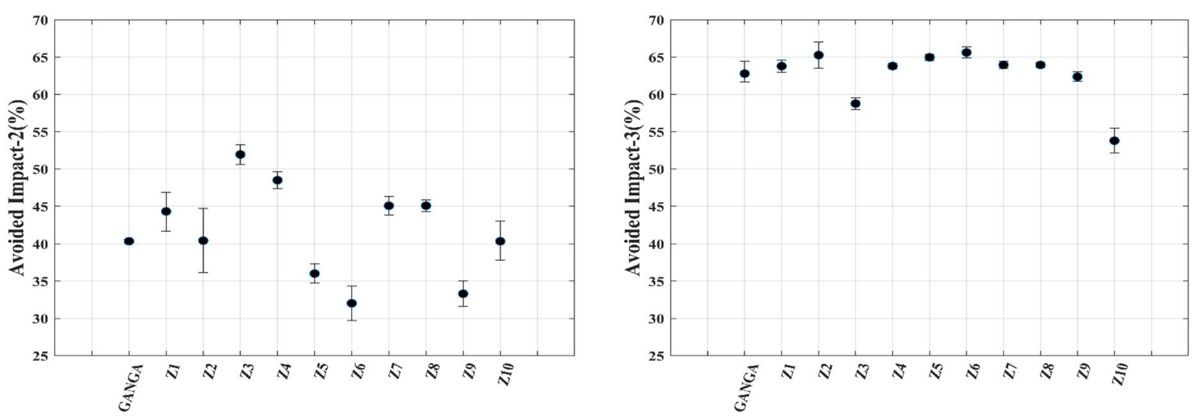

Fig. 7 Projected avoided impact of population exposure over Ganga River Basin and agro-climatic zones. solid circles represent the mean value of the exposure to TXX, and the bars show 10- and 90-percentile values derived from bootstrapping

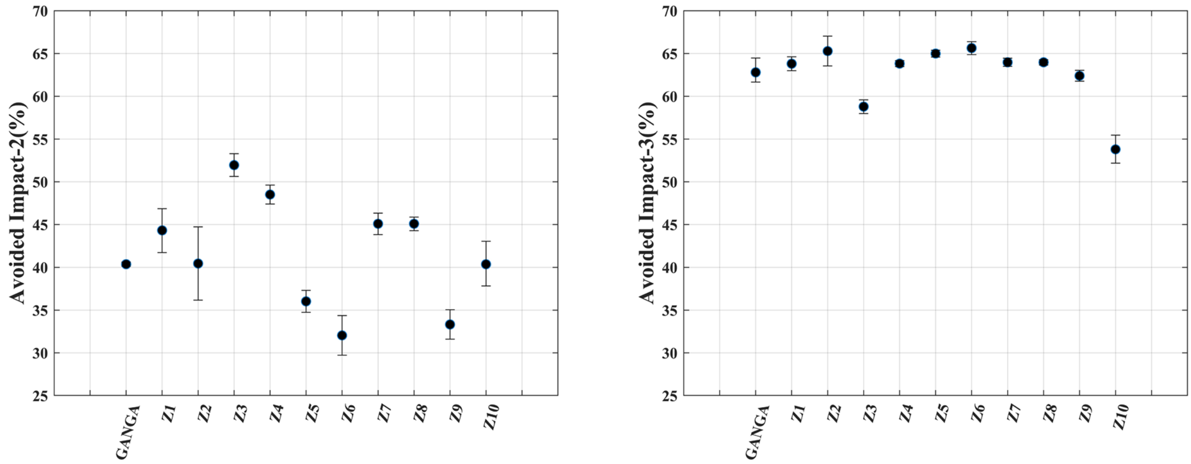

Fig. 8 Projected avoided impact areal exposure over Ganga River Basin and agro-climatic zones. Solid circles represent the mean value of the areal exposure, and the bars show 10- and 90-percentile values derived from bootstrapping

As shown in Fig. 7, about 46.99% and 52.16% of the population in the Ganga River Basin will be exposed to extreme temperature events (maximum temperature) once in 20 years respectively under 2 °C and 3 °C GWLs. In the present study, we have calculated the avoided impacts concerning global warming levels for all four SSPs. Results show that Zone-1 and Zone-2 are highly exposed to extreme temperature events of about 57.27% and 66.65% of populations, respectively, for AI-3, while 44.46% and 44.57% for AI-2. Zone-4 and Zone-5 show the lowest population exposure to extreme temperature events for both AI-2 and AI-3.

If we go for the areal exposure (Fig. 8) of the extreme temperature (maximum temperature) for the GRB, it was found that 40.36% area is exposed to AI-2 and 62.79% exposed to AI-3. Zone-9 exhibits a minimal area of about 32.04% exposed to TXX for AI-2 while Zone-3 reveals a maximum value of about 51.95%. Moving to AI-3, zones 2 and 6 shows higher values of areal exposure of around 65.27% and 65.63%, respectively, while zones 3 and 10 show minimum exposure of TXX to about 58.78 and 53.79% of the entire GRB.

Discussion and conclusion

Our findings show how temperature and precipitation extremes and frequency over GRB would vary as the world warms by 1.5, 2, and 3 °C. The outcomes of the study also show the impact averted by restricting the GWL to 2 °C rather than 3 °C, as well as the area and population exposure owing to forecasted extreme temperature and precipitation events. Climate simulations and future climate change estimates contain uncertainties (Diallo et al., 2012; Li et al., 2016), which have frequently been a limiting factor, particularly on regional and local scales. The daily maximum and minimum temperatures have been showing a trend of increasing over time, which could be an indication of a warming climate and could be the reason for a range of adverse environmental, economic, and social impacts (Dashkhuu et al., 2015). The outcomes of the study over GRB show that TNN is increasing at a rapid pace (almost more than double) compared to TXX, which indicates that the severity of cold events is decreasing while increasing in the case of hot events throughout the basin. The severity of warm night occurrences (TN90P) is increasing as compared to the warm day frequencies (TX90P), which indicates that rate of change in minimum temperature extremes has been happening faster than the rate of change of maximum temperature extremes as previously observed by Dash and Mamgain (2011), Panda et al. (2014), Revadekar et al. (2012), Skansi et al. (2013), and Rusticucci and Zazulie (2021). In case of daytime extremes (TXX and TX90P), driving changes are significantly associated with anthropogenic factors, whereas the natural environmental factors (water vapor and radiative feedbacks) have a stronger impact on nighttime extremes (TNN and

TN90P). This is the probable reason why nighttime extremes are showing larger warming trends than daytime extremes, as similar outcomes were also reported by Zhang et al. (2011a, b), Zhou and Ren (2011), Peng et al. (2017), Fan et al. (2022), and Simolo and Corti (2022). Consecutive dry and wet days both show increasing behavior over the entire basin which shows that extreme precipitation events are showing dominant behavior over the entire GRB and are consistent with an excessive estimation of total precipitation (PCPTOT) (Sharma & Goyal, 2020).

To assess the frequency of dry and wet spells in the research area, duration-based indices such as consecutive dry days (CDD) and consecutive wet days (CWD) have been evaluated. A decreasing trend has been observed in the study region for the absence of rainfall which is indicated by CDD as similar to the studies in Israel (Ziv et al., 2014) and Egypt (Donat et al., 2013); meanwhile, CWD has been reported showing a significant increasing trend for all the three scenarios (Sheikh et al., 2015). The findings of the study reveal that there is heterogeneity in the extreme precipitation indices, this is probably because of the variability in the physiographical features of the basin, as the elevation in the basin ranges between 8 and 7798 m from the mean sea level. Researchers and farmers should take this into account because it raises the demand for crop water, which in turn puts more strain on the GRB aquifer, which is already over-exploited. Our findings are consistent with the previous research carried out based on CMIP5 and CMIP6 models (Koteswara Rao et al., 2022; Gulizia et al., 2022; Gupta et al., 2020; Almazroui et al., 2020; Li et al., 2020). Zone-1 (Western Himalayan Region) was found to be highly affected by the extreme weather and climatic conditions as results are changing drastically throughout the zone with an increase in the level of warming. Since Zone-1 mostly has glacier covers and higher elevation physiography, therefore, due to higher vulnerability, any small changes in the behavior of the climate might lead to an increase in extreme events (Maurya et al., 2023; Shafq et al., 2019). Zone-1 is highly susceptible to the emission of the GHGs, which may lead to the rise in the mean temperature and probably be responsible for reduced glacial cover. The whole GRB experiences increased population exposure from 46.99 to 52.16% once every 20 years for AI-2 to AI-3, respectively.

Overall, as global warming progresses, changes in the magnitudes of precipitation and temperature-related extreme events are expected to increase significantly with the greatest growth occurring beneath 3 °C GWL in the whole domain and across all agro-climatic zones in the basin.

This study provides a scientific basis for policy-making. Actions should be taken at both regional and global scales to mitigate the negative effects of global warming-induced climate extremes. Effective actions must be taken at the global level to minimize global warming by reducing greenhouse gas emissions. This research has significant implications for achieving the 2015 Paris Agreement's worldwide emission reduction goals. The outcome of the study provides a noteworthy focus on agriculture and water resource management as well as adaptation and mitigation strategies for reducing the socioeconomic implications of climate extremes on a regional scale.

Acknowledgements We acknowledge Mishra et al. (2020b) for providing the bias-corrected CMIP6 dataset for India. We also extend our sincere gratitude to IMD-Pune, India, for providing the open-access rainfall gridded dataset and SEDAC for a higher-resolution population dataset.

Author contributions Harsh Vardhan Singh: data curation, formal analysis, methodology, investigation, visualization, and writing—original draft. Nitin Joshi: conceptualization, supervision, resources, validation, and writing—review and editing. Shakti Suryavanshi: supervision, investigation, and writing—review and editing.

Data availability We have obtained the observed data for the study region of rainfall from the India Meteorological Department (https://www.imdpune.gov.in) and temperature data have been acquired from Terrestrial Hydrology Group at Princeton University (Sheffield et al., 2006). The bias-corrected GCM datasets were obtained under different SSPs provided by Mishra et al. (2020) at https://doi.org/10.5281/zenodo.3874046. The population dataset is available under different SSPs from year 2000 to 2100 at NASA Socioeconomic Data and Applications Center (SEDAC).

Declarations

Ethical approval All authors have read, understood, and have complied as applicable with the statement on "Ethical responsibilities of Authors" as found in the Instructions for Authors.

Competing interests The authors declare no competing interests.

References

Adhikari, U., Nejadhashemi, A. P., & Woznicki, S. A. (2015). Climate change and eastern Africa: A review of impact on major crops. *Food and Energy Security, 4*(2), 110–132.

Akinsanola, A. A., Kooperman, G. J., Pendergrass, A. G., et al. (2020). Seasonal representation of extreme precipitation indices over the United States in CMIP6 present-day simulations. *Environmental Research Letters, 15*, 94003.

Akinsanola, A. A., Ongoma, V., & Kooperman, G. J. (2021). Evaluation of CMIP6 models in simulating the statistics of extreme precipitation over Eastern Africa. *Atmospheric Research, 254*(7), 105509. https://doi.org/10.1016/j.atmosres.2021.105509

Almazroui, M., Saeed, S., Saeed, F., Islam, M. N., & Ismail, M. (2020). Projections of precipitation and temperature over the South Asian countries in CMIP6. *Earth Systems and Environment, 4*, 297–320.

Ayugi, B., Zhihong, J., Zhu, H., Ngoma, H., Babaousmail, H., Rizwan, K., & Dike, V. (2021). Comparison of CMIP6 and CMIP5 models in simulating mean and extreme precipitation over East Africa. *International Journal of Climatology, 41*(15), 6474–6496.

Bhatt, D., Mall, R. K., Raju, K. N. P., & Suryavanshi, S. (2022). Multivariate drought analysis for the temperature homogeneous regions of India: lessons from the Gomati River basin. *Meteorological Applications, 29*(2), 1. https://doi.org/10.1002/met.2044

Burke, M., Hsiang, S. M., & Miguel, E. (2015). Global non-linear effect of temperature on economic production. *Nature, 527*(7577), 235–239.

Carleton, T. A. & Hsiang, S. M. (2016). Social and economic impacts of climate. *Science*, *353*(6304).

Chang-Fung-Martel, J., Harrison, M. T., Rawnsley, R., Smith, A. P., & Meinke, H. (2017). The impact of extreme climatic events on pasture-based dairy systems: A review. *Crop and Pasture Science, 68*(12), 1158–1169.

Chaubey, P. K., Mall, R. K., Jaiswal, R., & Payra, S. (2022). Spatio-temporal changes in extreme rainfall events over different Indian river basins. *Earth and Space Science, 9*(3), 285.

Chen, H., & Sun, J. (2019). Increased population exposure to extreme droughts in China due to 0.5 C of additional warming. *Environmental Research Letters, 14*(6), 064011.

Chen, H., & Sun, J. (2020). Increased population exposure to precipitation extremes in China under global warming scenarios. *Atmospheric and Oceanic Science Letters, 13*(1), 63–70.

Chen, H., & Sun, J. (2021). Significant increase of the global population exposure to increased precipitation extremes in the future. *Earth's Future, 9*(9), e2020EF001941.

Cheng-Zhi, C., Cong-Jian, L., Dan, X., Xiao-Shan, Z., & Jin, Z. (2021). Global warming and world soybean yields. *Journal of Agrometeorology, 23*(4), 367–374.

Chhogyel, N., & Kumar, L. (2018). Climate change and potential impacts on agriculture in Bhutan: A discussion of pertinent issues. *Agriculture & Food Security, 7*(1), 79.

Cogato, A., Meggio, F., De Antoni Migliorati, M., & Marinello, F. (2019). Extreme weather events in agriculture: A systematic review. *Sustainability, 11*(9), 2547.

Collins, M., Knutti, R., Arblaster, J., Dufresne, J. L., Fichefet, T., Friedlingstein, P., Gao, X., Gutowski, W. J., Johns, T., Krinner, G., & Shongwe, M. (2013). Long-term climate change: projections, commitments and irreversibility. In *Climate Change 2013-The Physical Science Basis: Contribution of Working Group I to the Fifth Assessment Report of the Intergovernmental Panel on Climate Change* (pp. 1029–1136). Cambridge University Press.

Dagar, V., Khan, M. K., Alvarado, R., Usman, M., Zakari, A., Rehman, A., & Tillaguango, B. (2021). Variations in technical efficiency of farmers with distinct land size across agro-climatic zones: evidence from India. *Journal of Cleaner Production, 315*, 128109. https://doi.org/10.1016/j.jclepro.2021.128109

Das, J., Manikanta, V., & Umamahesh, N. V. (2022). Population exposure to compound extreme events in India under different emission and population scenarios. *Science of the Total Environment, 806*, 150424.

Dash, S. K., & Mamgain, A. (2011). Changes in the frequency of different categories of temperature extremes in India. *Journal of Applied Meteorology and Climatology, 50*(9), 1842–1858.

Dashkhuu, D., Kim, J. P., Chun, J. A., & Lee, W. S. (2015). Long-term trends in daily temperature extremes over Mongolia. *Weather and Climate Extremes, 8*, 26–33.

Dell, M., Jones, B. F., & Olken, B. A. (2008). *Climate change and economic growth: evidence from the last half century* (No. w14132). National Bureau of Economic Research.

Dell, M., Jones, B. F., & Olken, B. A. (2012). Temperature shocks and economic growth: Evidence from the last half century. *American Economic Journal: Macroeconomics, 4*(3), 66–95.

Demertzis, K., & Iliadis, L. (2018). The impact of climate change on biodiversity: the ecological consequences of invasive species in Greece. In *Handbook of climate change communication: Vol. 1* (pp. 15–38). Springer, Cham.

Deshpande, N. R., Kothawale, D. R., & Kulkarni, A. (2016). Changes in climate extremes over major river basins of India. *International Journal of Climatology, 36*(14), 4548–4559. https://doi.org/10.1002/joc.4651

Diallo, I., Sylla, M. B., Giorgi, F., et al. (2012). Multimodel GCM-RCM ensemble-based projections of temperature and precipitation over west Africa for the early 21st century. *Int. J. Geophys., 2012*, 1–19. https://doi.org/10.1155/2012/972896

Diffenbaugh, N. S., & Burke, M. (2019). Global warming has increased global economic inequality. *Proceedings of the National Academy of Sciences, 116*(20), 9808–9813.

Diffenbaugh, N. S., Pal, J. S., Trapp, R. J., & Giorgi, F. (2005). Fine-scale processes regulate the response of extreme events to global climate change. *Proceedings of the National Academy of Sciences, 102*(44), 15774–15778.

Donat, M. G., Alexander, L. V., Yang, H., Durre, I., Vose, R., & Caesar, J. (2013). Global land-based datasets for monitoring climatic extremes. *Bulletin of the American Meteorological Society, 94*(7), 997–1006. https://doi.org/10.1175/BAMS-D-12-00109.1

Dosio, A., Mentaschi, L., Fischer, E. M., & Wyser, K. (2018). Extreme heat waves under 1.5 C and 2 C global warming. *Environmental Research Letters, 13*(5), 054006.

Eyring, V., Bony, S., Meehl, G. A., Senior, C. A., Stevens, B., Stouffer, R. J., & Taylor, K. E. (2016). Overview of the Coupled Model Intercomparison Project Phase 6 (CMIP6) experimental design and organization. *Geoscientific Model Development, 9*(5), 1937–1958. https://doi.org/10.5194/gmd-9-1937-2016

Fan, X., Duan, Q., Shen, C., Wu, Y., & Xing, C. (2022). Evaluation of historical CMIP6 model simulations and future projections of temperature over the Pan-Third Pole region. *Environmental Science and Pollution Research,* 1–16.

FAO. (1983). *World food security: A reappraisal of the concepts and approaches*. Director Generals Report.

Frame, D., Joshi, M., Hawkins, E., Harrington, L. J., & de Roiste, M. (2017). Population-based emergence of unfamiliar climates. *Nature Climate Change, 7*(6), 407–411. https://doi.org/10.1038/nclimate3297

Gao, J. (2020). Global 1-km downscaled population base year and projection grids based on the shared socioeconomic pathways, revision 01. *Palisades, New York: NASA Socioeconomic Data and Applications Center (SEDAC).* https://doi.org/10.7927/q7z9-9r69

Gulizia, C. N., Raggio, G. A., Camilloni, I. A., & Saurral, R. I. (2022). Changes in mean and extreme climate in southern South America under global warming of 1.5° C, 2° C, and 3° C. *Theoretical and Applied Climatology, 150*(1–2), 787–803.

Gupta, V., Singh, V., & Jain, M. K. (2020). Assessment of precipitation extremes in India during the 21st century under SSP1–1.9 mitigation scenarios of CMIP6 GCMs. *Journal of Hydrology, 590*, 125422.

Haan, C. (1977). *Statistical methods in hydrology*. Iowa StateUniversityPress.

Haines, A., Kovats, R. S., Campbell-Lendrum, D., & Corvalán, C. (2006). Climate change and human health: Impacts, vulnerability and public health. *Public Health, 120*(7), 585–596.

Handmer, J., Honda, Y., Kundzewicz, Z. W., Arnell, N., Benito, G., Hatfield, J., Mohamed, I. F., Peduzzi, P., Wu, S., Sherstyukov, B., & Takahashi, K. (2012). Changes in impacts of climate extremes: human systems and ecosystems. In *Managing the risks of extreme events and disasters to advance climate change adaptation special report of the intergovernmental panel on climate change* (pp. 231–290). Intergovernmental Panel on Climate Change.

Ibn Musah, A. A., Du, J., BilaliibUdimal, T., & AbubakariSadick, M. (2018). The nexus of weather extremes to agriculture production indexes and the future risk in Ghana. *Climate, 6*(4), 86.

IPCC. (2022). Climate change 2022: Impacts, adaptation, and vulnerability. In H.-O. Pörtner, D. C. Roberts, M. Tignor, E. S. Poloczanska, K. Mintenbeck, A. Alegría, M. Craig, S. Langsdorf, S. Löschke, V. Möller, A. Okem, & B. Rama (Eds.), *Contribution of Working Group II to the Sixth Assessment Report of the Intergovernmental Panel on Climate Change* (p. 3056). Cambridge, UK and New York, NY, USA: Cambridge University Press. https://doi.org/10.1017/9781009325844

Iyakaremye, V., Zeng, G., Yang, X., Zhang, G., Ullah, I., Gahigi, A., & Ayugi, B. (2021). Increased high-temperature extremes and associated population exposure in Africa by the mid-21st century. *Science of The Total Environment, 790*, 148162.

Jones, B., & O'Neill, B. C. (2016). Spatially explicit global population scenarios consistent with the Shared Socioeconomic Pathways. *Environmental Research Letters, 11*(8), 084003.

Jones, B., O'Neill, B. C., McDaniel, L., McGinnis, S., Mearns, L. O., & Tebaldi, C. (2015). Future population exposure to US heat extremes. *Nature Climate Change, 5*(7), 652–655.

Katopodis, T., Sfetsos, A., & Adamides, E. D. (2021). Vulnerability and impact assessment of extreme climate events in the Greek oil industry. In S*ustainable cities and resilience* (pp. 69–84). Singapore: Springer. https://doi.org/10.1007/978-981-16-5543-2_6

Koteswara Rao, K., Lakshmi Kumar, T. V., Kulkarni, A., Chowdary, J. S., & Desamsetti, S. (2022). Characteristic changes in climate projections over Indus Basin using the bias corrected CMIP6 simulations. *Climate Dynamics, 58*(11–12), 3471–3495.

Lee, O., Seo, J., Won, J., Choi, J., & Kim, S. (2021). Future extreme heat wave events using Bayesian heat wave intensity-persistence day-frequency model and their uncertainty. *Atmospheric Research, 255*(5), 105541.https://doi.org/10.1016/j.atmosres.2021.105541

Li, D., Zhou, T., Zou, L., Zhang, W., & Zhang, L. (2018). Extreme high-temperature events over East Asia in 1.5°C and 2°C warmer futures: Analysis of NCAR CESM low-warming experiments. *Geophysical Research Letters, 45*, 1541–1550. https://doi.org/10.1002/2017GL076753

Li, G., Xie, S., Du, Y., et al. (2016). Effects of excessive equatorial cold tongue bias on the projections of tropical Pacific climate change. Part I: The warming pattern in CMIP5 multi-model ensemble. *Climate Dynamics, 47*, 3817–3831. https://doi.org/10.1007/s00382-016-3043-5

Li, Z., Fang, G., Chen, Y., Duan, W., & Mukanov, Y. (2020). Agricultural water demands in Central Asia under 1.5° C and 2.0° C global warming. *Agricultural Water Management*, *231*, 106020.

Li, Z., Guo, X., Yang, Y., Hong, Y., Wang, Z., & You, L. (2019). Heatwave trends and the population exposure over China in the 21st century as well as under 1.5 C and 2.0 C global warmer future scenarios. *Sustainability, 11*(12), 3318.

Ma, F., & Yuan, X. (2021). Impact of climate and population changes on the increasing exposure to summertime compound hot extremes. *Science of the Total Environment, 772*, 145004.

Marx, A., Kumar, R., Thober, S., Rakovec, O., Wanders, N., Zink, M., Wood, E. F., Pan, M., Sheffield, J., & Samaniego, L. (2018). Climate change alters low flows in Europe under global warming of 1.5, 2, and 3 C. *Hydrology and Earth System Sciences, 22*(2), 1017–1032.

Maurya, H. K., Joshi, N., Swami, D., & Suryavanshi, S. (2023). Change in temperature extremes over India under 1.5° C and 2° C global warming targets. *Theoretical and Applied Climatology, 152*(1–2), 57–73.

Mechoso, C. R., Arakawa, A., & Angeles, L. (2015). General circulation models. Edisi Second Edition. Elsevier. Encyclopedia of Atmospheric Sciences.

Meehl, G. A., Zwiers, F., Evans, J., Knutson, T., Mearns, L., & Whetton, P. (2000). Trends in extreme weather and climate events: Issues related to modeling extremes in projections of future climate change. *Bulletin of the American Meteorological Society, 81*(3), 427–436.

Mendelsohn, R., Dinar, A., & Williams, L. (2006). The distributional impact of climate change on rich and poor countries. *Environment and development economics*, 159–178.

Mirza, M. M. Q. (2003). Climate change and extreme weather events: Can developing countries adapt? *Climate Policy, 3*(3), 233–248.

Mishra, P. K., Thayyen, R. J., Singh, H., Das, S., Nema, M. K., & Kumar, P. (2022). Assessment of cloudbursts, extreme rainfall and vulnerable regions in the Upper Ganga basin, Uttarakhand, India. *International Journal of Disaster Risk Reduction, 69*, 102744. https://doi.org/10.1080/02626667.2021.1976783

Mishra, V., Bhatia, U., & Tiwari, A. D. (2020a). Bias-corrected climate projections for South Asia from coupled model intercomparison project-6. *Scientific Data, 7*(1), 338.

Mishra, V., Bhatia, U., & Tiwari, A. D. (2020b). Bias corrected climate projections from CMIP6 models for South Asia. *Zenodo*. https://doi.org/10.5281/zenodo.3873998

Mitchell, D., Heaviside, C., Vardoulakis, S., Huntingford, C., Masato, G., Guillod, B. P., ... & Allen, M. (2016). Attributing human mortality during extreme heat waves to anthropogenic climate change. *Environmental Research Letters, 11*(7), 074006.

Mittal, N., Mishra, A., Singh, R., & Kumar, P. (2014). Assessing future changes in seasonal climatic extremes in the Ganges river basin using an ensemble of regional climate models. *Climatic Change, 123*(2), 273–286. https://doi.org/10.1007/s10584-014-1056-9

Mondal, S. K., Huang, J., Wang, Y., Su, B., Kundzewicz, Z. W., Jiang, S., ... & Jiang, T (2022). Changes in extreme precipitation across South Asia for each 0.5 °C of warming from 1.5 °C to 3.0 °C above pre-industrial levels. *In Atmospheric Research, 266*(1), 105961. https://doi.org/10.1016/j.atmosres.2021.105961

Moore, F. C., & Diaz, D. B. (2015). Temperature impacts on economic growth warrant stringent mitigation policy. *Nature Climate Change, 5*(2), 127.

Mora, C., Spirandelli, D., Franklin, E. C., Lynham, J., Kantar, M. B., Miles, W., Smith, C. Z., Freel, K., Moy, J., Louis, L. V., & Barba, E. W. (2018). Broad threat to humanity from cumulative climate hazards intensified by greenhouse gas emissions. *Nature Climate Change, 8*(12), 1062–1071.

Nangombe, S. S., Zhou, T., Zhang, W., Zou, L., & Li, D. (2019). High-temperature extreme events over Africa under 1.5 and 2 C of global warming. *Journal of Geophysical Research: Atmospheres, 124*(8), 4413–4428.

Nepal, S., & Shrestha, A. B. (2015). Impact of climate change on the hydrological regime of the Indus, Ganges and Brahmaputra river basins: A review of the literature. *International Journal of Water Resources Development, 31*(2), 201–218.

Orimoloye, I. R., Mazinyo, S. P., Kalumba, A. M., Ekundayo, O. Y., & Nel, W. (2019). Implications of climate variability and change on urban and human health: A review. *Cities, 91*, 213–223.

Pachauri, R. K., Allen, M. R., Barros, V. R., Broome, J., Cramer, W., Christ, R., Church, J. A., Clarke, L., Dahe, Q., Dasgupta, P., & Dubash, N. K. (2014a). *Climate change 2014a: synthesis report. Contribution of Working Groups I, II and III to the fifth assessment report of the Intergovernmental Panel on Climate Change* (p. 151). IPCC.

Pachauri, R. K., Meyer, L. A., & IPCC,. (2014b). *Climate change 2014: Synthesis report. Contribution of Working Groups I, II and III to the fifth assessment report of the Intergovernmental Panel on Climate Change* (p. 151). IPCC.

Panagoulia, D., Economou, P., & Caroni, C. (2014). Stationary and nonstationary generalized extreme value modelling of extreme precipitation over a mountainous area under climate change. *Environmetrics, 25*(1), 29–43.

Panda, D. K., Mishra, A., Kumar, A., Mandal, K. G., Thakur, A. K., & Srivastava, R. C. (2014). Spatiotemporal patterns in the mean and extreme temperature indices of India, 1971–2005. *International Journal of Climatology, 34*(13), 3585–3603.

Parain, E. C., Rohr, R. P., Gray, S. M., & Bersier, L. F. (2019). Increased temperature disrupts the biodiversity–ecosystem functioning relationship. *The American Naturalist, 193*(2), 227–239.

Parey, S., Hoang, T. T. H., & Dacunha-Castelle, D. (2010). Different ways to compute temperature return levels in the climate change context. *Environmetrics, 21*(7–8), 698–718.

Peng, X., She, Q., Long, L., Liu, M., Xu, Q., Zhang, J., & Xiang, W. (2017). Long-term trend in ground-based air temperature and its responses to atmospheric circulation and anthropogenic activity in the Yangtze River Delta, China. *Atmospheric Research, 195*, 20–30.

Perera, A. T. D., Nik, V. M., Chen, D., Scartezzini, J. -L., & Hong, T. (2020). Quantifying the impacts of climate change and extreme climate events on energy systems. *Nature Energy, 5*(2), 150–159. https://doi.org/10.1038/s41560-020-0558-0

Planton, S., Déqué, M., Chauvin, F., & Terray, L. (2008). Expected impacts of climate change on extreme climate events. *ComptesRendus Geoscience, 340*(9–10), 564–574. https://doi.org/10.1016/j.crte.2008.07.009

Pörtner, H. -O., Roberts, D. C., Tignor, M., Poloczanska, E. S., Mintenbeck, K., Alegría, A., Craig, M., Langsdorf, S., Löschke, S., Möller, V., Okem, A., & Rama, B. (2022). Climate change 2022: impacts, adaptation, and vulnerability. Contribution of working group ii to the sixth assessment report of the intergovernmental panel on climate change. Cambridge University Press.

Pretis, F., Schwarz, M., Tang, K., Haustein, K., & Allen, M. R. (2018). Uncertain impacts on economic growth when stabilizing global temperatures at 1.5 C or 2 C warming. *Philosophical Transactions of the Royal Society A: Mathematical, Physical and Engineering Sciences*, *376*(2119), 20160460.

Rahman, R., & Zafarullah, H. (2020). Impact of climate change on human health: Adaptation challenges in Queensland. *Australia. Climate Research, 80*(1), 59–72.

Rai, P. K., Singh, G. P., & Dash, S. K. (2020). Projected changes in extreme precipitation events over various subdivisions of India using RegCM4. *Climate Dynamics, 54*, 247–272.

Rani, S., Kumar, R., & Maharana, P. (2022). Climate change, its impacts, and sustainability issues in the Indian Himalaya: an introduction. In Climate Change (pp. 1–27). Springer, Cham.

Rao, K. K., Patwardhan, S. K., Kulkarni, A., Kamala, K., Sabade, S. S., & Kumar, K. K. (2014). Projected changes in mean and extreme precipitation indices over India using PRECIS. *Global and Planetary Change, 113*, 77–90.

Reddy, N. M., & Saravanan, S. (2023). Extreme precipitation indices over India using CMIP6: A special emphasis on the SSP585 scenario. *Environmental Science and Pollution Research, 30*(16), 47119–47143.

Revadekar, J. V., Kothawale, D. R., Patwardhan, S. K., Pant, G. B., & Rupa Kumar, K. (2012). About the observed and future changes in temperature extremes over India. *Natural Hazards, 60*, 1133–1155.

Rohat, G., Flacke, J., Dosio, A., Dao, H., & van Maarseveen, M. (2019). Projections of human exposure to dangerous heat in African cities under multiple socioeconomic and climate scenarios. *Earth's Future, 7*(5), 528–546.

Russo, S., Sillmann, J., Sippel, S., Barcikowska, M. J., Ghisetti, C., Smid, M., & O'Neill, B. (2019). Half a degree and rapid socioeconomic development matter for heatwave risk. *Nature Communications, 10*(1), 136. https://doi.org/10.1038/s41467-018-08070-4

Rusticucci, M., & Zazulie, N. (2021). Attribution and projections of temperature extreme trends in South America based on CMIP5 models. *Ann N Y Acad Sci n/a*. https://doi.org/10.1111/nyas.14591

Schleussner, C.-F., Lissner, T. K., Fischer, E. M., Wohland, J., Perrette, M., Golly, A., Rogelj, J., Childers, K., Schewe, J., Frieler, K., Mengel, M., Hare, W., & Schaeffer, M. (2016). Differential climate impacts for policy-relevant limits to global warming: The case of 1.5 °C and 2 °C. *Earth System Dynamics, 7*, 327–351. https://doi.org/10.5194/esd-7-327-2016

Sen Roy, S., & Balling, R. C., Jr. (2004). Trends in extreme daily precipitation indices in India. *International Journal of Climatology: A Journal of the Royal Meteorological Society, 24*(4), 457–466.

Seneviratne, S., Nicholls, N., Easterling, D., Goodess, C., Kanae, S., Kossin, J., Luo, Y., Marengo, J., McInnes, K., Rahimi, M., & Reichstein, M. (2012). Changes in climate extremes and their impacts on the natural physical environment. A Special Report of Working Groups I and II of the Intergovernmental Panel on Climate Change (IPCC). Cambridge University Press, Cambridge, UK, and New York, NY, USA, pp. 109–230.

Shafq, M. U., Rasool, R., Ahmed, P., & Dimri, A. P. (2019). Temperature and precipitation trends in Kashmir valley, north western Himalayas. *Theoretical and Applied Climatology, 135*, 293–304. https://doi.org/10.1007/s00704-018-2377-9

Sharma, A., & Goyal, M. K. (2020). Assessment of the changes in precipitation and temperature in Teesta River basin in Indian Himalayan Region under climate change. *Atmospheric Research, 231*, 104670.

Sheffield, J., Goteti, G., & Wood, E. F. (2006). Development of a 50-year high-resolution global dataset of meteorological forcings for land surface modeling. *Journal of Climate, 19*(13), 3088–3111.https://doi.org/10.1175/JCLI3790.1

Sheikh, M. M., Manzoor, N., Ashraf, J., Adnan, M., Collins, D., Hameed, S. L. S. M., ... & Shrestha, M. L. (2015). Trends in extreme daily rainfall and temperature indices over South Asia. *International Journal of Climatology, 35*(7), 1625–1637.

Siddha, S., & Sahu, P. (2022). Impact of climate change on the river ecosystem. In Ecological significance of river ecosystems (pp. 79–104). Elsevier.

Simolo, C., & Corti, S. (2022). Quantifying the role of variability in future intensification of heat extremes. *Nature Communications, 13*(1), 7930.

Singh, R., & Kumar, R. (2019). Climate versus demographic controls on water availability across India at 1.5 C, 2.0 C and 3.0 C global warming levels. *Global and Planetary Change, 177*, 1–9.

Skansi, M. D. L. M., Brunet, M., Sigró, J., et al. (2013). Warming and wetting signals emerging from analysis of changes in climate extreme indices over South America. *Glob Planet Change, 100*, 295–307. https://doi.org/10.1016/j.gloplacha.2012.11.004

Smale, D. A., Wernberg, T., Oliver, E. C., Thomsen, M., Harvey, B. P., Straub, S. C., Burrows, M. T., Alexander, L. V., Benthuysen, J. A., Donat, M. G., & Feng, M. (2019). Marine heatwaves threaten global biodiversity and the provision of ecosystem services. *Nature Climate Change, 9*(4), 306–312.

Smirnov, O., Zhang, M., Xiao, T., Orbell, J., Lobben, A., & Gordon, J. (2016). The relative importance of climate change and population growth for exposure to future extreme droughts. *Climatic Change, 138*(1), 41–53.

Stillman, J. H. (2019). Heat waves, the new normal: Summertime temperature extremes will impact animals, ecosystems, and human communities. *Physiology, 34*(2), 86–100.

Strauss, F., Formayer, H., & Schmid, E. (2013). High resolution climate data for Austria in the period 2008–2040 from a statistical climate change model. *International Journal of Climatology, 33*(2), 430–443.

Sun, Q., Miao, C., Hanel, M., Borthwick, A. G., Duan, Q., Ji, D., & Li, H. (2019). Global heat stress on health, wildfires, and agricultural crops under different levels of climate warming. *Environment International, 128*, 125–136.

Swarnkar, S., Prakash, S., Joshi, S. K., & Sinha, R. (2021). Spatio-temporal rainfall trends in the Ganga River Basin over the last century: understanding feedback and hydrological impacts. *Hydrological Sciences Journal, 66*(14), 2074–2088. https://doi.org/10.1080/02626667.2021.1976783

Thayyen, R. J., Mishra, P. K., Jain, S. K., Wani, J. M., Singh, H., Singh, M. K., & Yadav, B., (2021). Hanging glacier avalanche (Raunthigad - Rishiganga) and debris flow disaster of 7th February 2021, Uttarakhand, India, a preliminary assessment. https://doi.org/10.21203/rs.3.rs-340429/v1

The Global Climate: 2011–15, United Nations Framework Convention on Climate Change. (2016). ISBN: 978–92–63–11179–1.

Tirado, M. C., Clarke, R., Jaykus, L. A., McQuatters-Gollop, A., & Frank, J. M. (2010). Climate change and food safety: a review. *Food Research International, 43*(7), 1745–1765.A

Tong, S., & Ebi, K. (2019). Preventing and mitigating health risks of climate change. *Environmental Research, 174*, 9–13.

Tuholske, C., Caylor, K., Funk, C., Verdin, A., Sweeney, S., Grace, K., ... & Evans, T. (2021). Global urban population exposure to extreme heat. *Proceedings of the National Academy of Sciences, 11*8(41), e2024792118.

Urama, N. E., Eboh, E. C., & Onyekuru, A. (2019). Impact of extreme climate events on poverty in Nigeria: A case of the 2012 flood. *Climate and Development, 11*(1), 27–34. https://doi.org/10.1080/17565529.2017.1372267

Vasseur, D. A., DeLong, J. P., Gilbert, B., Greig, H. S., Harley, C. D., McCann, K. S., Savage, V., Tunney, T. D., & O'Connor, M. I. (2014). Increased temperature variation poses a greater risk to species than climate warming. *Proceedings of the Royal Society B: Biological Sciences, 281*(1779), 20132612.

Vautard, R., Gobiet, A., Sobolowski, S., Kjellström, E., Stegehuis, A., Watkiss, P., Mendlik, T., Landgren, O., Nikulin, G., Teichmann, C., & Jacob, D. (2014). The European climate under a 2° C global warming. *Environmental Research Letters, 9*(3), 034006.

Vogel, E., Donat, M. G., Alexander, L. V., Meinshausen, M., Ray, D. K., Karoly, D., Meinshausen, N., & Frieler, K. (2019). The effects of climate extremes on global agricultural yields. *Environmental Research Letters, 14*(5), 054010.

Weber, T., Bowyer, P., Rechid, D., Pfeifer, S., Raffaele, F., Remedio, A. R., Teichmann, C., & Jacob, D. (2020). Analysis of compound climate extremes and exposed population in Africa under two different emission scenarios. *Earth's Future, 8*(9), e2019EF001473.

Yadav, B. C., Thayyen, R. J., & Jain, K. (2020). Topoclimatic zones and characteristics of the upper Ganga basin, Uttarakhand, India. *International Journal of Climatology, 40*(14), 6002–6019.

Yehia, A .G., Fahmy, K. M., Mehany, M. A. S., & Mohamed, G. G. (2017). Impact of extreme climate events on water supply sustainability in Egypt: case studies in Alexandria region and Upper Egypt. *Journal of Water and Climate Change, 8*(3), 484–494. https://doi.org/10.2166/wcc.2017.111

Yin, J., Guo, S., Wang, J., Chen, J., Zhang, Q., Gu, L., ... & Zhang, Y. (2023). Thermodynamic driving mechanisms for the formation of global precipitation extremes and ecohydrological effects. *Science China Earth Sciences, 66*(1), 92–110.

Yosef, Y., Aguilar, E., & Alpert, P. (2019). Changes in extreme temperature and precipitation indices: Using an innovative daily homogenized database in Israel. *International Journal of Climatology, 39*(13), 5022–5045.

Yue, S., & Pilon, P. (2004). A comparison of the power of the t test, Mann-Kendall and bootstrap tests for trend detection/Une comparaison de la puissance des tests t de Student, de Mann-Kendall et du bootstrap pour la détection de tendance. *Hydrological Sciences Journal, 49*(1), 21–37.

Yue, Y., Yan, D., Yue, Q., Ji, G., & Wang, Z. (2021). Future changes in precipitation and temperature over the Yangtze River Basin in China based on CMIP6 GCMs. *Atmospheric Research, 264*, 105828.

Zhan, Y. J., Ren, G. Y., Shrestha, A. B., Rajbhandari, R., Ren, Y. Y., Sanjay, J., ... & Wang, S. (2017). Changes in extreme precipitation events over the Hindu Kush Himalayan region during 1961–2012. *Advances in Climate Change Research, 8*(3), 166–175.

Zhang, Q., Li, J., David Chen, Y., & Chen, X. (2011a). Observed changes of temperature extremes during 1960–2005 in China: Natural or human-induced variations? *Theoretical and Applied Climatology, 106*, 417–431.

Zhang, W., Zhou, T., Zou, L., Zhang, L., & Chen, X. (2018). Reduced exposure to extreme precipitation from 0.5 °C less warming in global land monsoon regions. *Nature Communications, 9*(1), 3153. https://doi.org/10.1038/s41467-018-05633-3

Zhang, X., Alexander, L., Hegerl, G. C., Jones, P., Tank, A. K., Peterson, T. C., ... & Zwiers, F. W. (2011b). Indices for monitoring changes in extremes based on daily temperature and precipitation data. *Wiley Interdisciplinary Reviews: Climate Change, 2*(6), 851–870.

Zhao, W., Chou, J., Li, J., Xu, Y., Li, Y., & Hao, Y. (2022). Impacts of extreme climate events on future rice yields in global major rice-producing regions. *International journal of environmental research and public health, 19*(8).https://doi.org/10.3390/ijerph19084437

Zhou, Y., & Ren, G. (2011). Change in extreme temperature event frequency over mainland China, 1961–2008. *Climate Research, 50*(2–3), 125–139.

Ziv, B., Saaroni, H., Pargament, R., Harpaz, T., & Alpert, P. (2014). Trends in rainfall regime over Israel, 1975–2010, and their relationship to large-scale variability. *Regional Environmental Change, 14*(5), 1751–1764. https://doi.org/10.1007/s10113-013-0414-x